The flaky Co_3O_4/BCNO composite as an efficient and stable catalyst for oxygen reduction reaction

Yintao Zhang[a], Zehao Zang[a], Xiang Li[b,*], Ping Yang[a], Junfang Zhang[a], Lanlan Li[a], Xiaofei Yu[a], Xiaojing Yang[a], Zunming Lu[a], Xinghua Zhang[a,c,*]

[a]School of Materials Science and Engineering, Hebei University of Technology, Tianjin 300130, China
[b]Graduate School, Hebei University of Technology, Tianjin 300130, China
[c]Hebei Key Lab Boron Nitride Micro & Nano Mat, Hebei University of Technology, Tianjin 300130, China
*Email: lixiang@hebut.edu.cn, zhangxinghua@hebut.edu.cn

Supporting Information

Electrochemical measurements

Electrochemical measurements were performed using a rotating disk electrode instrument (RRDE-3A) equipped with an electrochemical workstation (CHI 760E). Using a three-electrode system, a glassy carbon electrode (3 mm in diameter) coated with the prepared catalyst was served as the working electrode, the graphite rod was used as the counter electrode to form the current loop, and the saturated calomel electrode (SCE) was used as the reference electrode. The catalyst ink was prepared by mixing 2.5 mg catalyst, 2.5 mg acid-washed Ketjen black (conductive agent), 500 μL isopropanol, 465 μL deionized water, and 35 μL of 5 wt% Nafion membrane solution, followed by ultrasonic dispersion for 30 min. The surface of the glassy carbon electrode was first polished to a bright state, and then the catalyst ink (6.4 μL) was dropped on the glassy carbon disc electrode, and then dried at room temperature.

Cyclic voltammetry (CV) curves were recorded at a scan rate of 50 mV s^{-1} in O_2 (N_2)-saturated 0.1 M KOH electrolyte. Before measuring the polarization curves, repeat the cyclic voltammetry pretreatment for several cycles until a stable curve is obtained and then perform linear

voltammetry (LSV) at 5 mV s^{-1}, 1600 rpm and sweep from 0 V to 1.2 V (vs RHE). Electrochemical impedance spectroscopy (EIS) data were collected in the frequency range of 0.1-1000000 Hz using the electrochemical workstation. The electrochemical active surface area (ECSA) was obtained by cyclic voltammetry measurements in 0.1 M KOH electrolyte at different scan rates (2 mV s^{-1}, 4 mV s^{-1}, 6 mV s^{-1}, 8 mV s^{-1}, 10 mV s^{-1}) in the non-Faraday region (1.0-1.1 V vs RHE). The accelerated durability tests (adt) were carried out in 0.6-1.0 V (vs RHE) for 10 k cycles with a scan rate of 100 mV s^{-1}.

The electron transfer number is mainly obtained by the rotating disk electrode experiment according to the Koutecky–Levich equation as follows:

$$1/j=1/j_K+1/j_L \quad \text{(eq. 1)}$$

where $j_L=0.62nFAC_0D^{2/3}w^{1/2}V^{-1/6}$. The electron transfer number n can be obtained from the above equation. j is the measured current density, j_k is the kinetic density, and j_L is the diffusion-limited current density. In addition, n, F, A, C_0, D, w, and V are the number of transferred electrons, Faraday constant (96485C mol^{-1}), electrode geometric specific surface area, oxygen concentration in 0.1 M KOH electrolyte ($C_0=1.26\times10^{-3}$ mol cm^{-3}), diffusion coefficient (1.9×10^{-5} $cm^2\cdot s^{-1}$), electrode rotation angular velocity (rad$\cdot s^{-1}$) and solution viscosity (v=0.01 $cm^2\cdot s^{-1}$), respectively.

Electron transfer number and hydrogen peroxide yield can also be measured by rotating ring disk electrode (RRDE).

$$H_2O_2\%=\frac{200IR/N}{ID+IR/N} \quad \text{(eq. 2)}$$

$$n=\frac{4ID}{ID+IR/N} \quad \text{(eq. 3)}$$

where ID is the disk current density, IR is the ring current density, and N is the ring complement coefficient, generally 0.37.

The corrosion current was obtained by Tafel extrapolation. The schematic diagram is shown in **Fig. R1**. In corrosion, by employing the SterneGeary equation, quantitative information about corrosion potentials along with corrosion currents can be obtained from the slope of the curves, as follows:

$$i_{corr} = \frac{1}{(2.303R_p)(\frac{\beta_a \times \beta_c}{\beta_a + \beta_c})} \quad \text{(eq. 4)}$$

Where i_{corr}, R_p, β_a, *and* β_c are the corrosion current density in amperes per square centimeter, the corrosion resistance in ohms square centimeter, the anodic Tafel slope in volts or millivolts per decade of current density, and the cathodic Tafel slope in volts or millivolts per decade of current density, respectively. The quantity $\frac{\beta_a \times \beta_c}{\beta_a + \beta_c}$ refers to the Tafel constant. We use the "Corrosion Rate Calculation" function in the "Analysis" module of the CHI760E electrochemical workstation to directly fit the corrosion current, as shown in **Fig. R1** to the Tafel polarization curve.

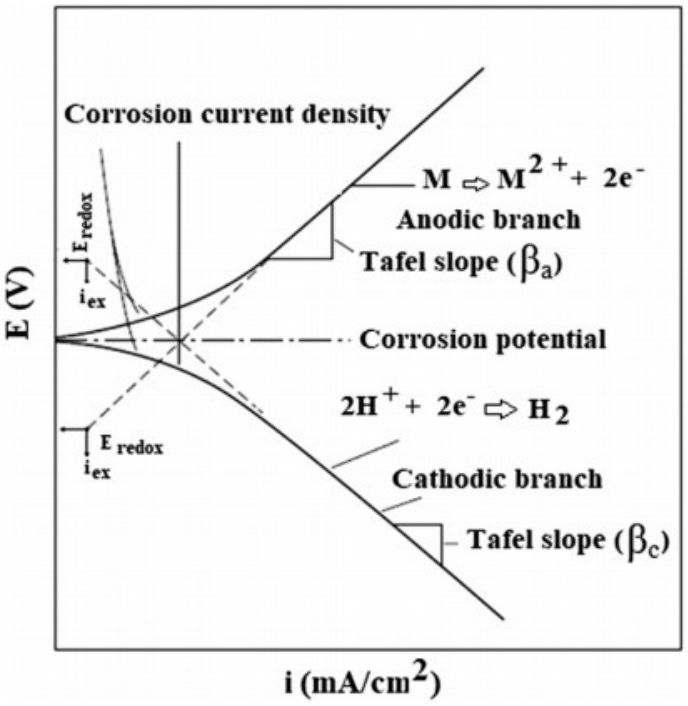

Fig. S1. Scheme of Tafel extrapolation[1]

Zn-air battery tests: The liquid Zn-air battery was made to evaluate battery performance, in which carbon fiber paper coated with Co_3O_4/BCNO catalysts was used as the air cathode, and the polished Zn plate was used as anode. The electrolyte of Zn-air battery was prepared by mixing 6.0 M KOH with 0.2 M zinc acetate. Catalyst ink was dropped on the hydrophobic carbon fiber paper with a loading amount of 1.0 mg cm^{-2} in order to prepare the air electrode. As a comparison, the commercial Pt/C catalyst was used with the same loading content.

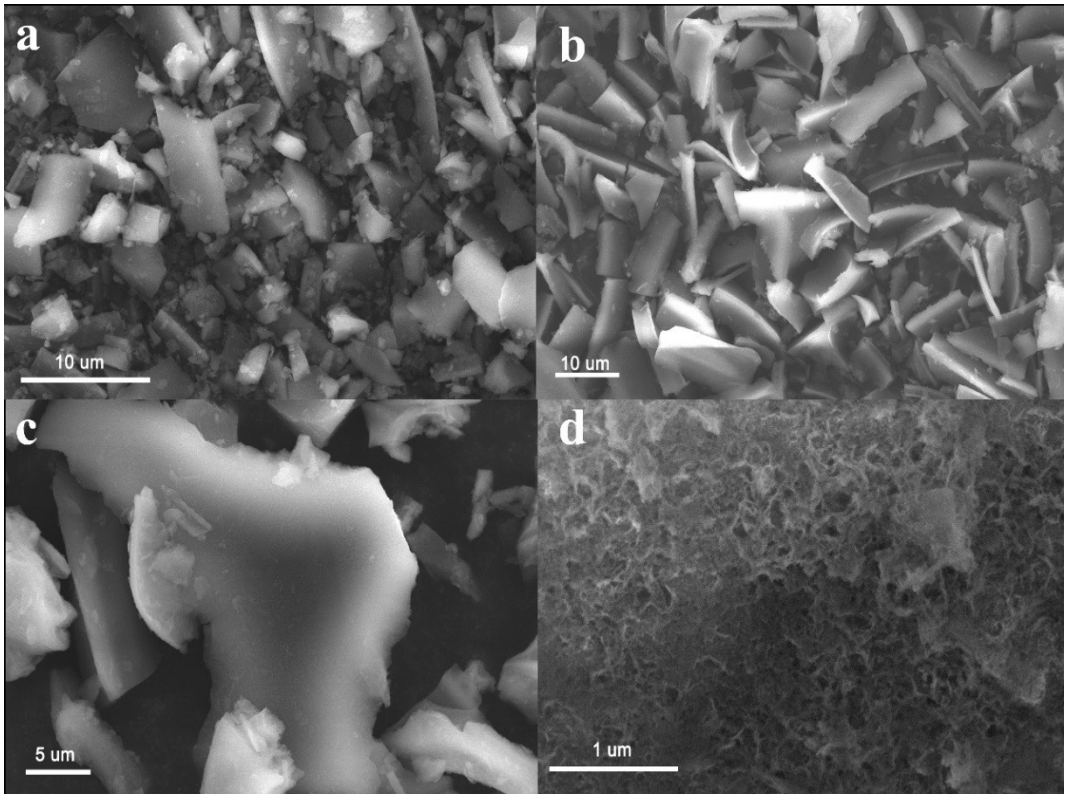

Fig. S1. SEM images of (a) BCNO and (b-d) Co_3O_4/BCNO catalysts.

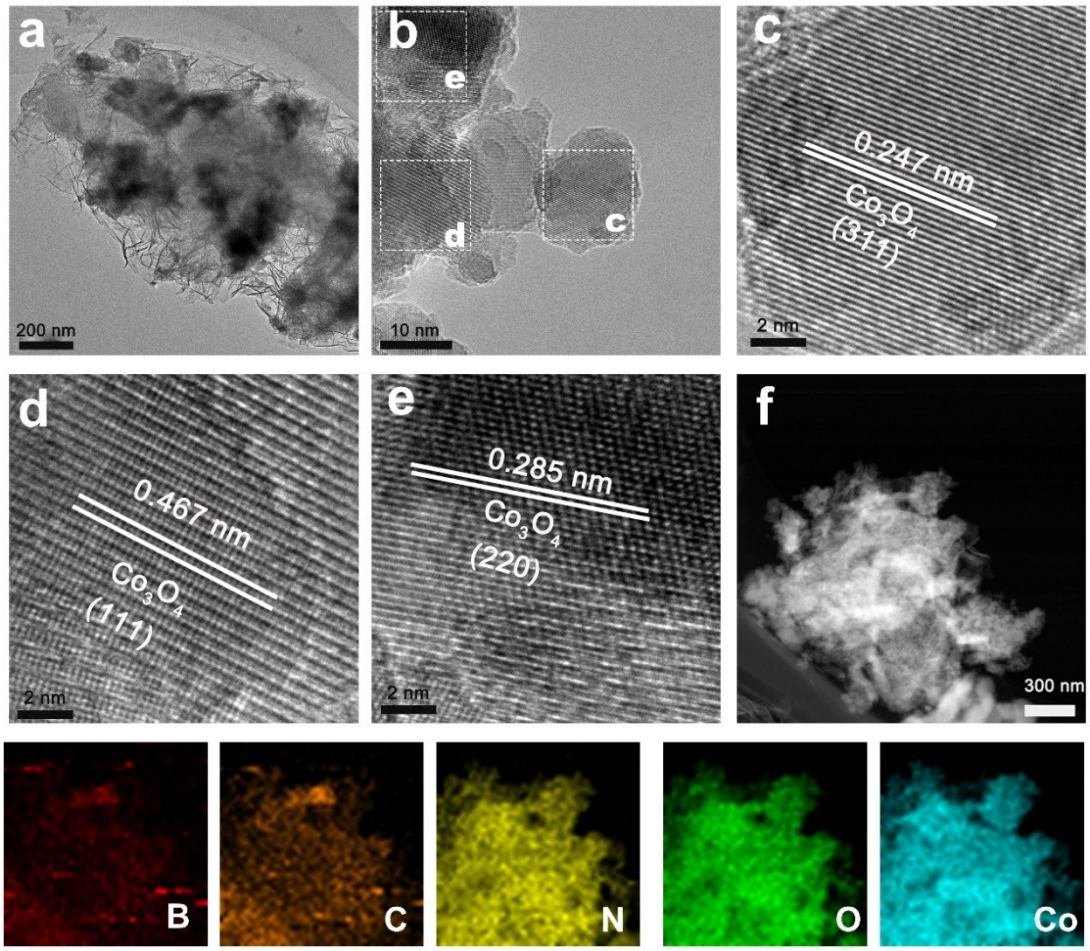

Fig. S2. (a) TEM image and (b-e) HRTEM images of acid washed Co_3O_4/BCNO composite, (f) TEM image and corresponding element mapping of B, C, N, O and Co elements for Co_3O_4/BCNO catalyst after acid washing.

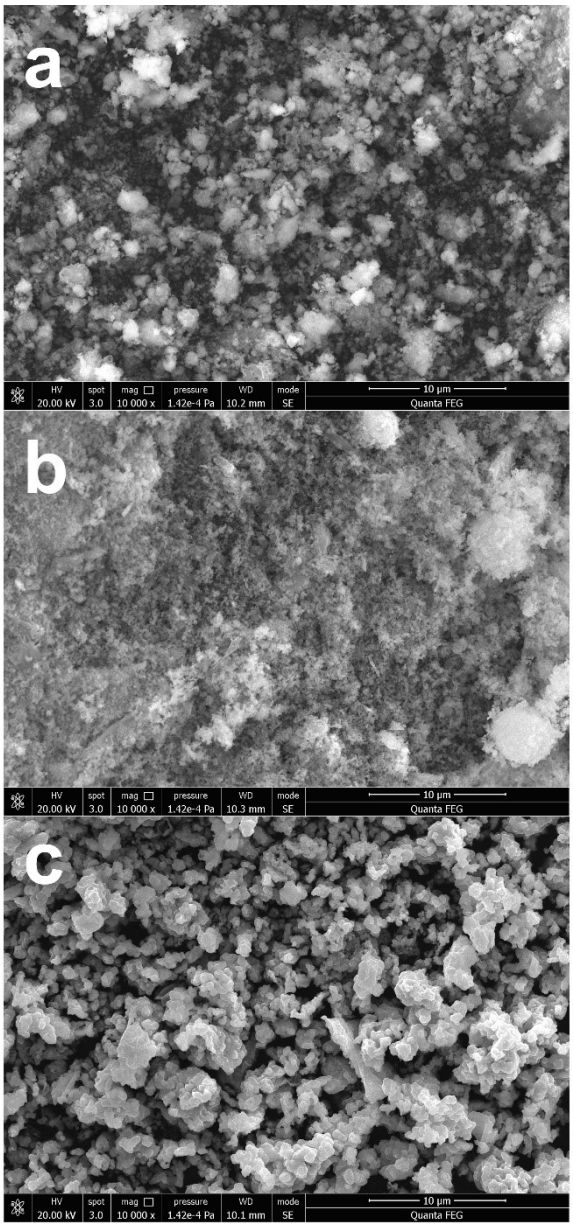

Fig. S3. SEM images of (a) Co_3O_4/BCO, (b) Co_3O_4/CNO and (c) Co_3O_4 catalysts.

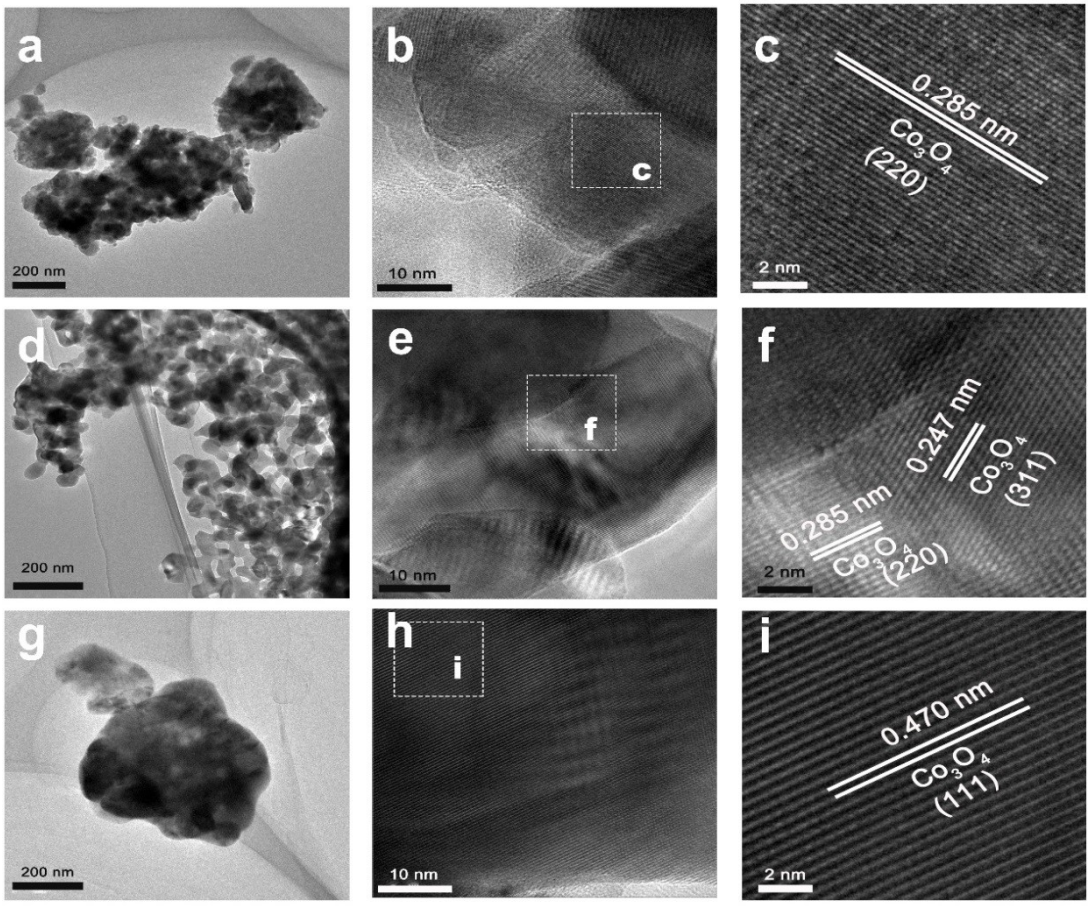

Fig. S4. (a) TEM image and (b-c) HRTEM images of Co_3O_4/BCO composite, (d) TEM image and (e-f) HRTEM images of Co_3O_4/CNO composite, (g) TEM image and (h-i) HRTEM images of Co_3O_4 catalysts.

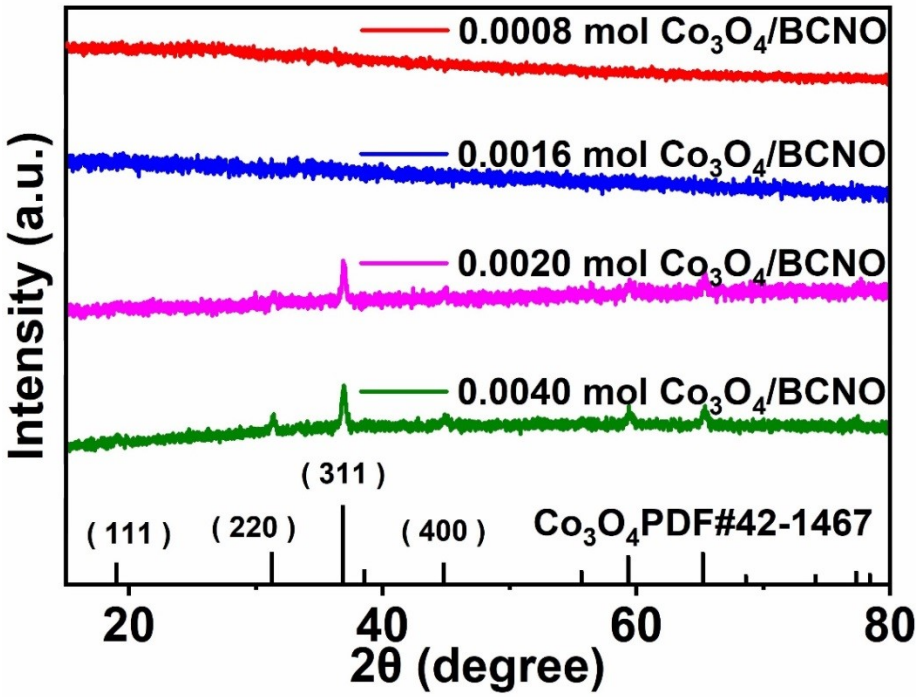

Fig. S5. XRD patterns of Co_3O_4/BCNO composites as the amount of cobalt acetate was increased to 0.0008, 0.0016, 0.002 and 0.004 mol.

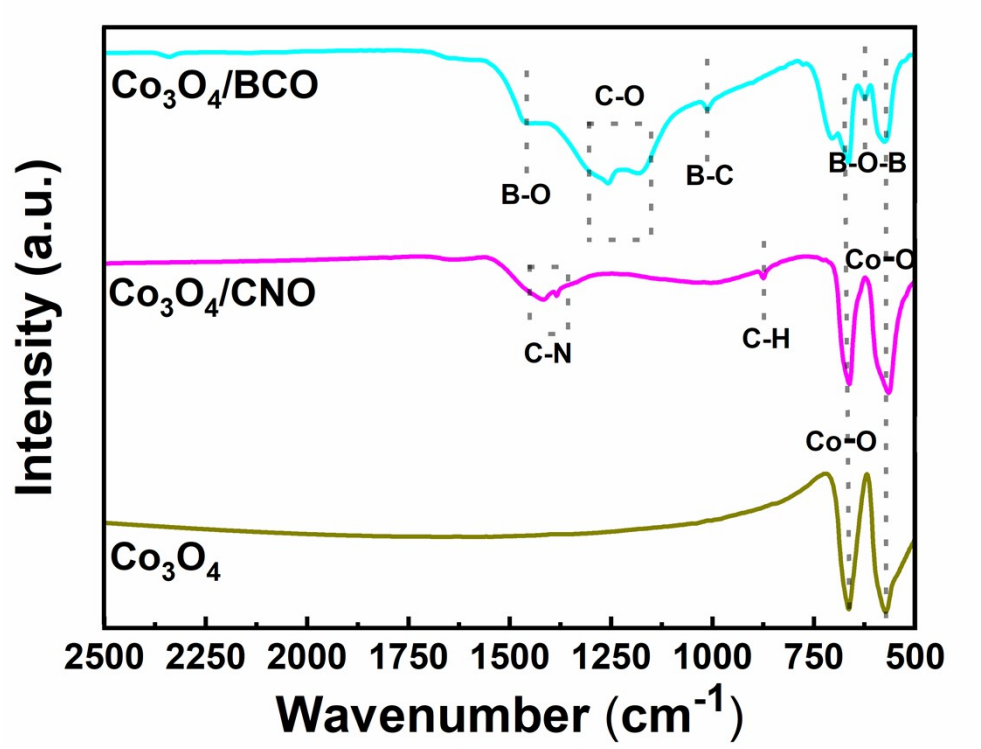

Fig. S6. FTIR spectra of Co_3O_4/BCO, Co_3O_4/CNO and Co_3O_4 catalysts.

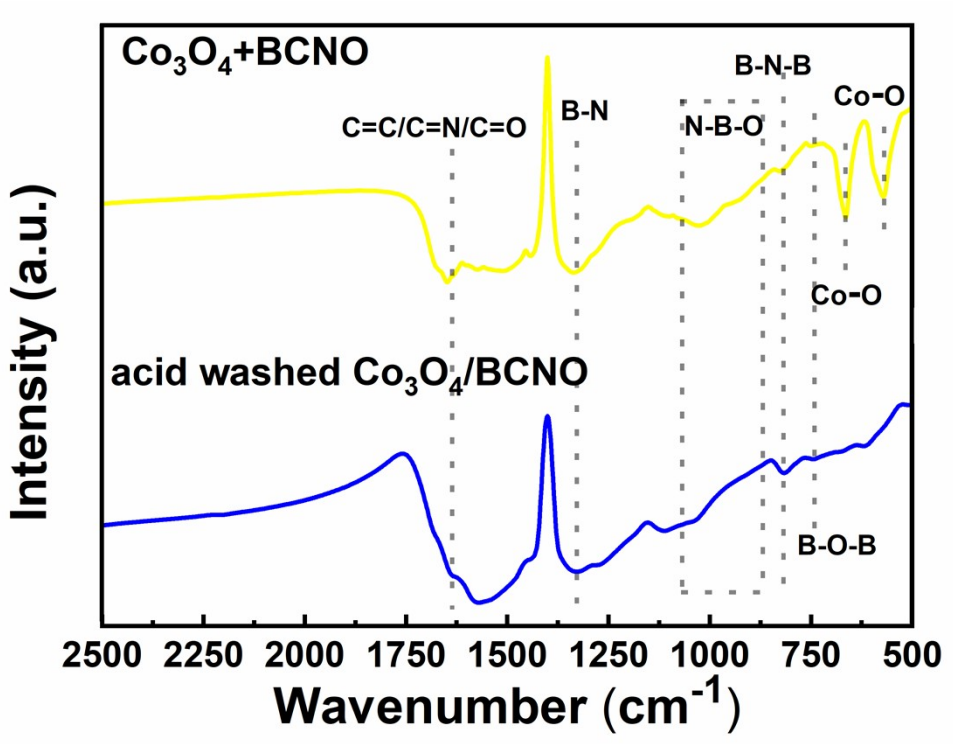

Fig. S7. FTIR spectra of Co_3O_4+BCNO and acid washed Co_3O_4/BCNO composite.

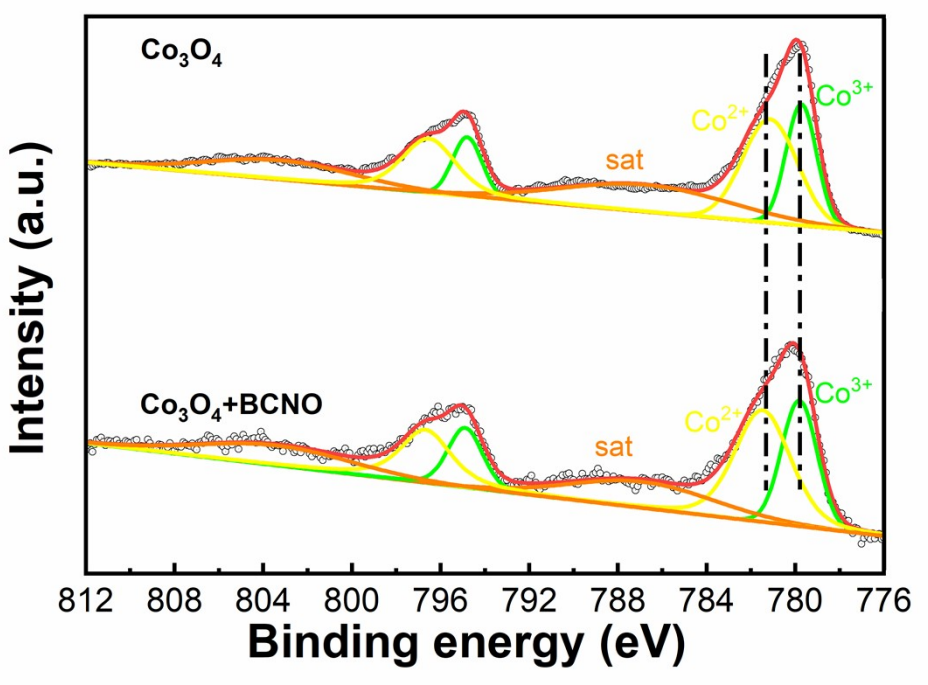

Fig. S8. Co 2p XPS spectra and fitting curves for Co_3O_4 and Co_3O_4+BCNO catalysts.

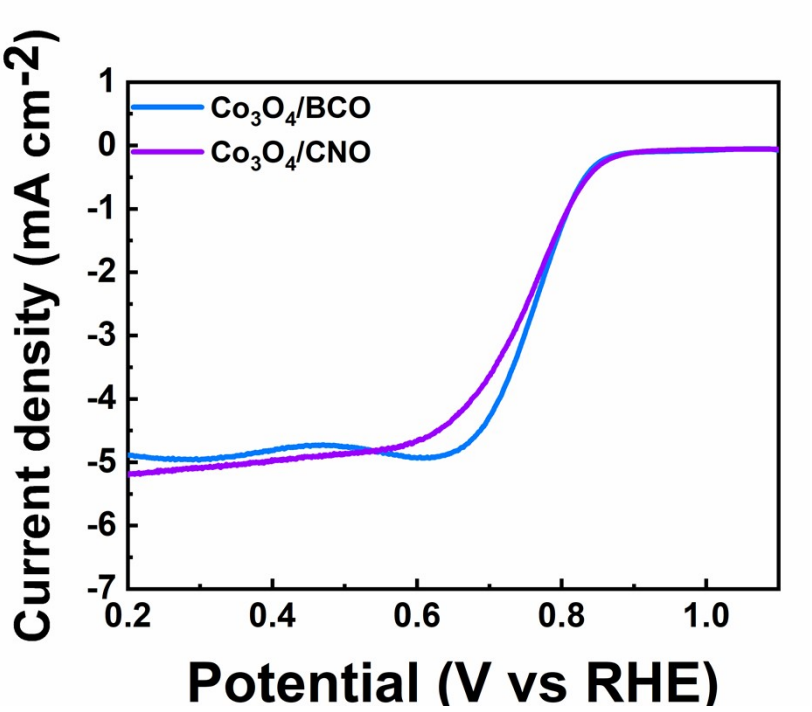

Fig. S9. LSV curves tested at 1600 rpm with a sweep rate of 5 mV s^{-1} for the Co_3O_4/BCO and Co_3O_4/CNO catalysts.

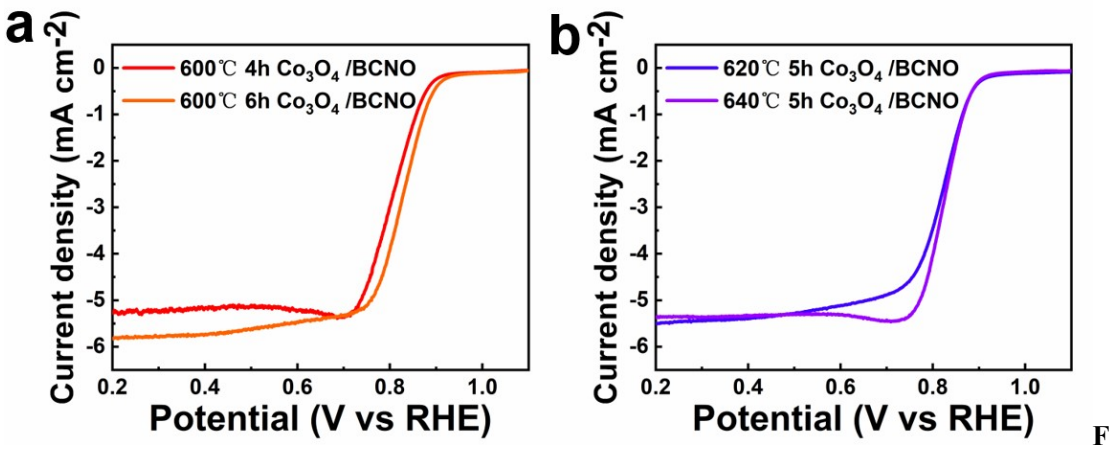

Fig. S10. LSV curves tested at 1600 rpm with a sweep rate of 5 mV s^{-1} of (a) the Co_3O_4/BCNO composite sintered at 600 ºC for 4 hours and 6 hours, (b) the Co_3O_4/BCNO composite prepared at 620 ºC and 640 ºC for 5 hours .

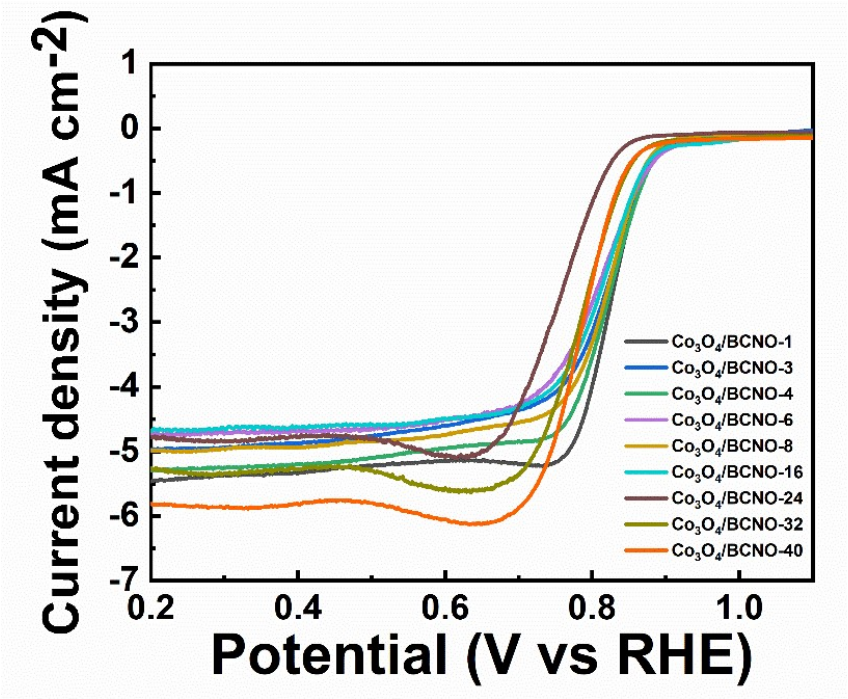

Fig. S11. LSV curves measured at 1600 rpm with a sweep rate of 5 mV s^{-1} for Co_3O_4/BCNO composites with different contents of Co source.

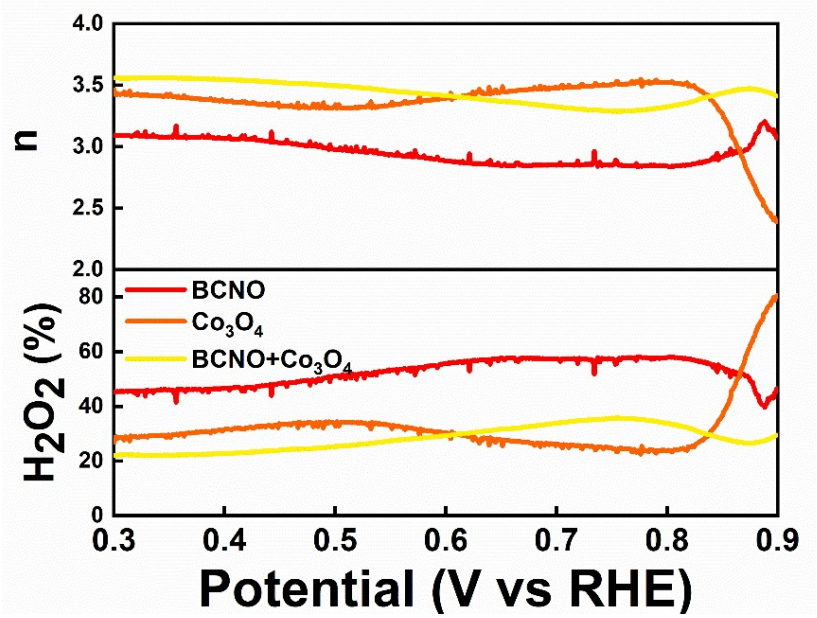

Fig. S12. Electron transfer number and H_2O_2 yield of BCNO, Co_3O_4 and BCNO+Co_3O_4 catalysts.

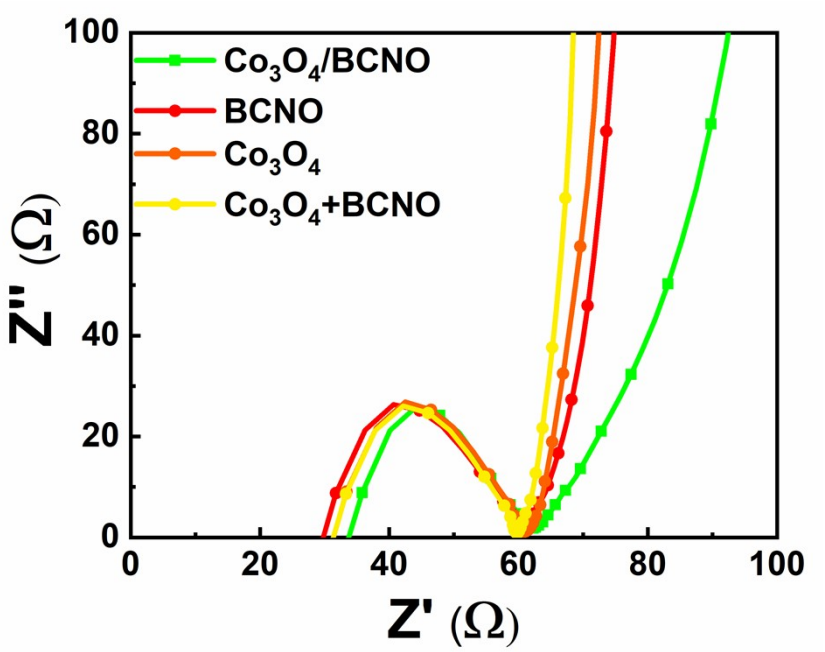

Fig. S13. Electrochemical impedance spectra of Co_3O_4/BCNO, BCNO, Co_3O_4 and BCNO+Co_3O_4 catalysts.

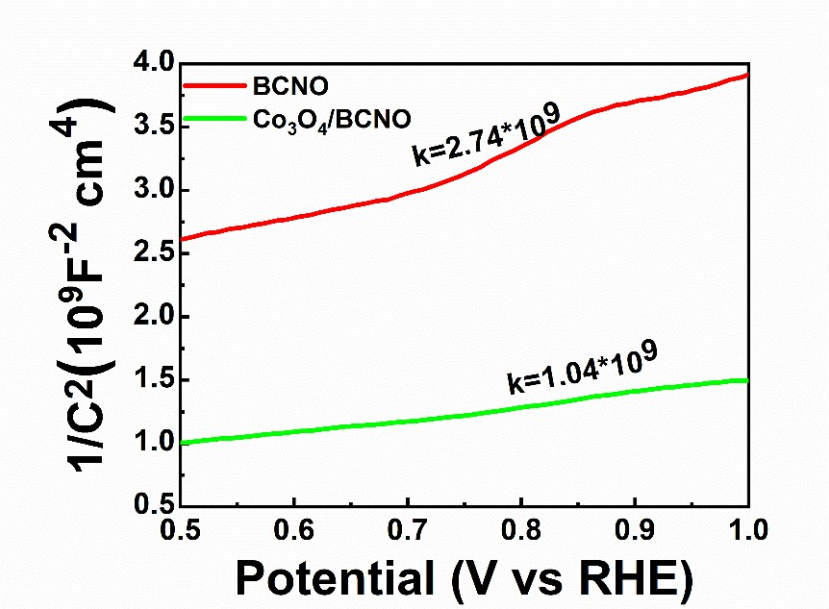

Fig.S14. Mott-Schottky plots of BCNO and Co_3O_4/BCNO samples.

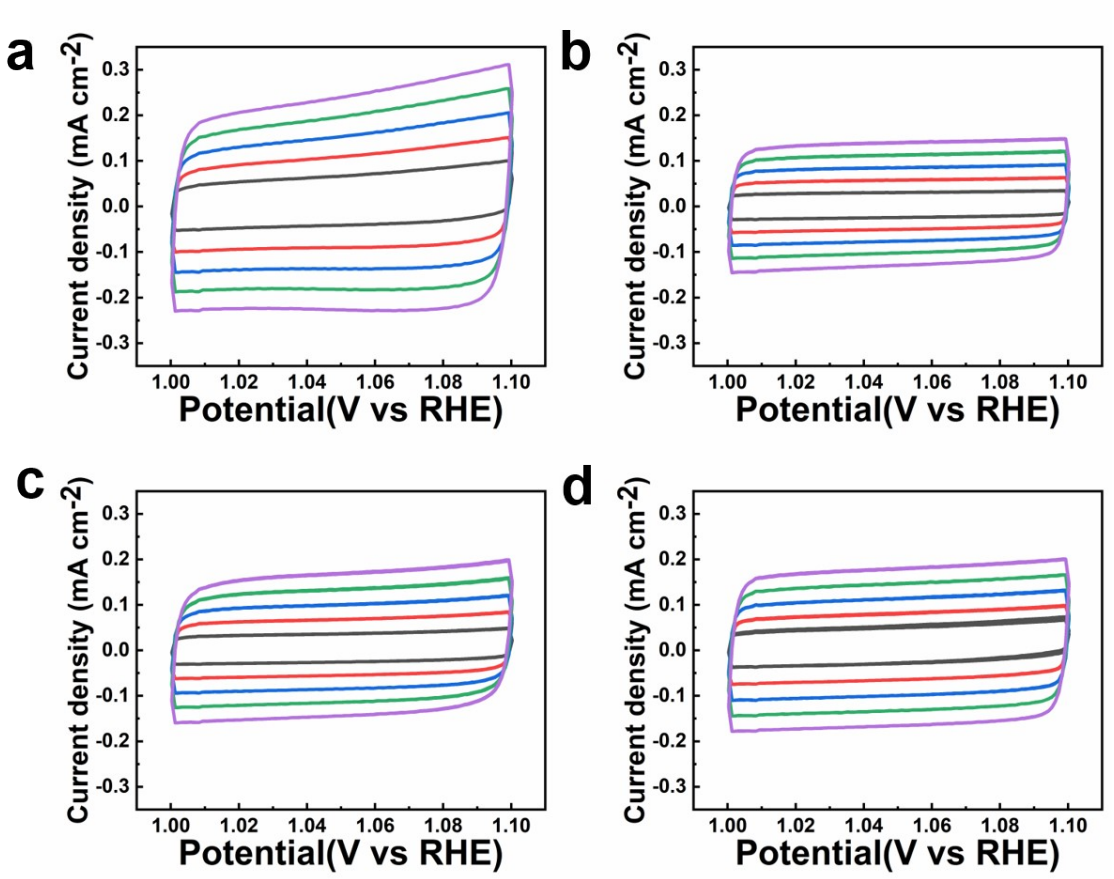

Fig. S15. CV curves of (a) Co_3O_4/BCNO, (b) BCNO, (c) Co_3O_4, (d) BCNO+Co_3O_4 at various scan rates within a non-Faraday potential range (1.0 V-1.1 V).

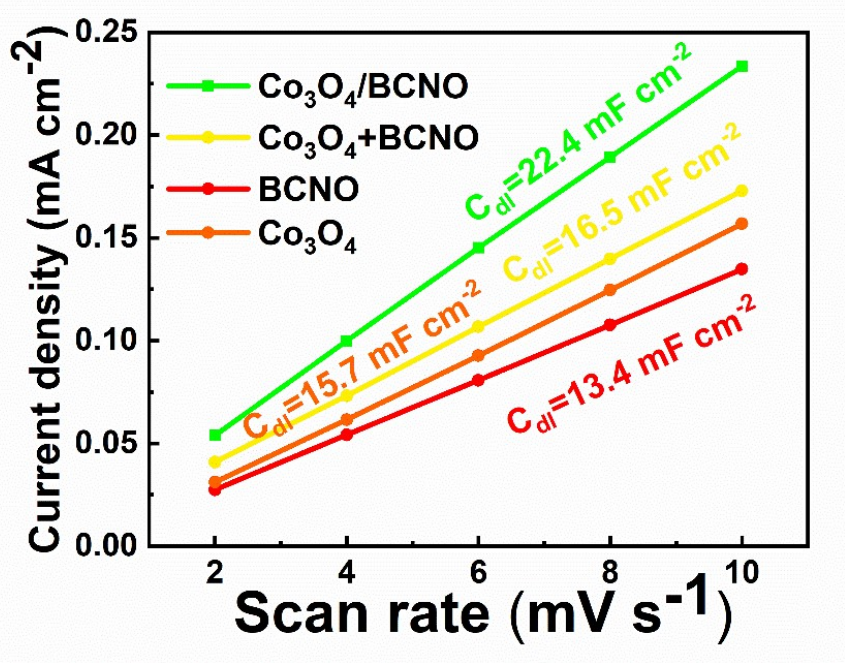

Fig. S16. Linear fitting results of capacitive currents vs. scan rate for different catalysts.

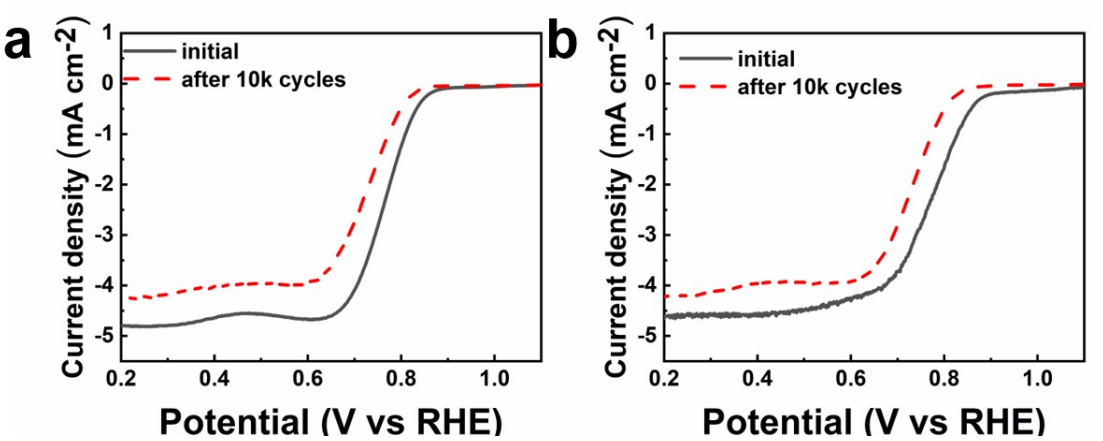

Fig. S17. LSV curves of (a) Co_3O_4, and (b) Co_3O_4+BCNO before and after 10000 potential cycles in O_2-saturated 0.1 M KOH solution.

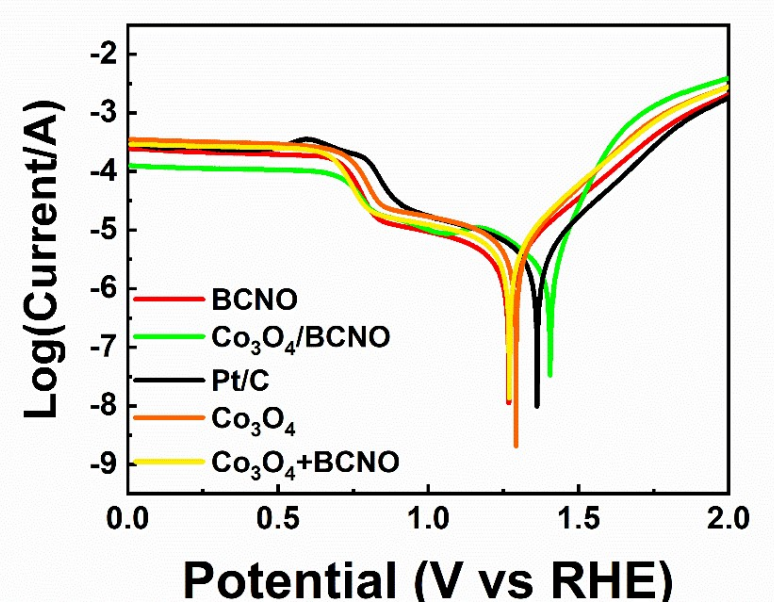

Fig. S18. Tafel polarization curves of Co_3O_4/BCNO, BCNO, Co_3O_4, BCNO+CO_3O_4 and Pt/C catalysts in O_2-saturated 0.1 M KOH solution.

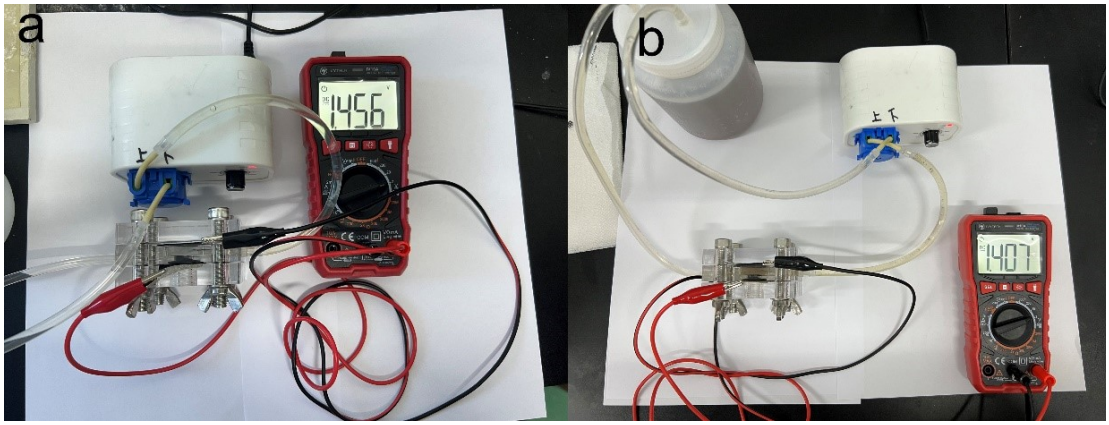

Fig. S19. Open circuit voltage photos of Zn-air batteries based on (a) Co_3O_4/BCNO composite and (b) Pt/C catalyst.

Table S1. Composition of BCNO and Co_3O_4/BCNO samples before and after ORR.

sample	B (%)	C (%)	N (%)	O (%)	Co (%)
BCNO	4.77	56.82	19.56	18.85	0
Surface of Co_3O_4/BCNO before ORR	3.21	58.15	12.72	20.78	5.14
Bulk of Co_3O_4/BCNO before ORR	8.29	54.45	13.41	17.85	6.00
Surface of Co_3O_4/BCNO after ORR	3.27	56.00	9.11	25.90	5.72
Bulk of Co_3O_4/BCNO after ORR	5.05	56.52	10.82	22.24	5.37

Table S2. Half-wave potentials of different Co_3O_4 based composite catalysts

Catalyst	$E_{1/2}$(V)	References
Co_3O_4/BCNO	0.84	This work
Co_3O_4-NP/N-rGO	0.76	[2]
0.5% Ce-Co_3O_4	0.665	[3]
Co_3O_4/N-CNTs	0.82	[4]
Co_3O_4/NOCS	0.82	[5]
Co_3O_4-C_3N_4/rGO	0.81	[6]
Co_3O_4/NCNTs/3D graphene	0.80	[7]
Co/Co_3O_4@NHCS	0.82	[8]
Co_3O_4/N-KC	0.82	[9]

Table S3. Half-wave potentials of Co_3O_4/BCNO composites with different contents of Co source.

Co source contents (mol)	$E_{1/2}$ (V)
0.0001	0.82
0.0002	0.84
0.0003	0.82
0.0004	0.81
0.0006	0.80
0.0016	0.80
0.0024	0.76
0.0032	0.79
0.0040	0.79

Table S4. Corrosion currents of Co_3O_4/BCNO, BCNO, Co_3O_4, BCNO+CO_3O_4 and Pt/C catalysts.

Catalysts	Corrosion current (A)
Co_3O_4/BCNO	$2.018*10^{-6}$
BCNO	$2.739*10^{-6}$
Co_3O_4	$4.688*10^{-6}$
BCNO+CO_3O_4	$4.004*10^{-6}$
Pt/C	$3.210*10^{-6}$

References

1. K. Kakaei, M. D. Esrafili and A. Ehsani, *Interface Sci. Technol.*, 2019, **27**, 303-337.
2. X. Han, G. He, Y. He, J. Zhang, X. Zheng, L. Li, C. Zhong, W. Hu, Y. Deng and T.-Y. Ma, *Adv. Energy Mater.*, 2018, **8**.4816-4824.
3. L. Wang, Q. Liu, N. Ta, H. Fan and E. Wang, *Chemistryselect*, 2021, **6**, 3512-3518.
4. A. Zhang, J. Wu, L. Xue, S. Yan and S. Zeng, *Inorg Chem*, 2020, **59**, 403-414.
5. Y. Wang, R. Gan, Z. Ai, H. Liu, C. Wei, Y. Song, M. Dirican, X. Zhang, C. Ma and J. Shi, *Carbon*, 2021, **181**, 87-98.
6. L. Gong, X. Li, Q. Zhang, B. Huang, Q. Yang, G. Yang and Y. Liu, *Appl. Surf. Sci.*, 2020, **525**.146624.
7. Y. Liu, L. Yang, B. Xie, N. Zhao, L. Yang, F. Zhan, Q. Pan, J. Han, X. Wang, J. Liu, J. Li and Y. Yang, *Chem. Eng. J.*, 2020, **381**.122681.
8. X. Wang, H. Gai, Z. Chen, Y. Liu, J. Zhang, B. Zhao, A. Toghan and M. Huang, *Mater. Today Energy*, 2020, **18**.100497.
9. G. Cheng, G. Liu, P. Liu, L. Chen, S. Han, J. Han, F. Ye, W. Song, B. Lan, M. Sun and L. Yu, *Front Chem*, 2019, **7**, 766.